MAGNETIC ARMOR AS A METHOD OF ANTITERROR PROTECTION OF OBJECTS AGAINST SHAPED-CHARGE ACTION

S.V. Fedorov[1], A.V. Babkin[1], S.V. Ladov[1], G. A. Shvetsov[2], and A. D. Matrosov[2]

[1] *Bauman Moscow State Technical University, Moscow, Russia*
[2]*Lavrentyev Institute of Hydrodynamics, Siberian Division of the Russian Academy of Sciences, Lavrentyev Prospekt 15, Novosibirsk, 630090, Russia, e-mail: shvetsov@hydro.nsc.ru*

Experiments have shown that the creation of a magnetic field in the liner of a shaped charge before its firing can considerably reduce the penetration capability of the shaped-charge jet. The present paper considers the possibility of using this effect for the antiterrorist protection of various objects against shaped-charge action.

INTRODUCTION

Experiments [1] have shown that the creation of an axial magnetic field in a shaped charge (SC) liner immediately before SC firing leads to a considerable reduction in the penetration capability of the shaped-charge jet (SCJ).

During the formation of a shaped-charge jet, the liner material ceases to move in the radial direction upon impingement on the charge axis and experiences enormous tensile deformations in the axial direction, i.e., along the magnetic field lines produced in the liner. In this case, the freezing-in effect should lead to magnetic-field generation and amplification directly in the material of the jet being formed. This process is accompanied by the occurrence of electromagnetic forces that push apart the SCJ, which can lead to jet breakup with radial scattering of the material and loss of the penetration capability [2].

Figure 1 illustrates the formation of a SCJ under implosion of a SCJ in the absence of a magnetic field and in the presence of an initial field of intensity $B_0 = 0.2$ T and $B_0 = 0.5$ T. It is seen that the presence of the magnetic field leads to radial scattering of the SCJ being formed. As noted above, this scattering is due to the powerful electromagnetic forces that arise in the SCJ material as a result of magnetic field "pumping." The SC operation failure effect in a magnetic field of fairly low intensity (a few tenths of a tesla) is of interest in terms of its practical application for the antiterrorist protection of various objects against shaped charges by means of “magnetic armor,” i.e., by the creation of a magnetic field ahead of an object subjected to shaped-charge attack.

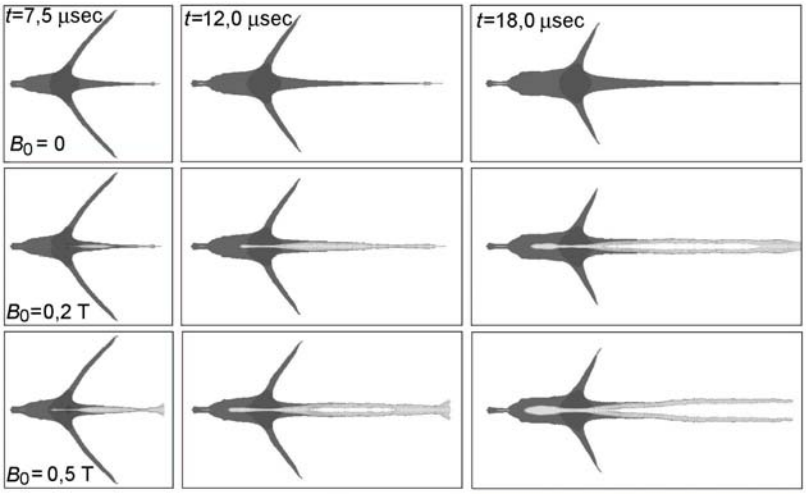

Figure 1. Magnetic-field effect on the formation of a shaped-charge jet.

A key point in the implementation of this method of protection is to ensure the penetration of a magnetic field of the required level in the shaped-charge warhead (SCW) liner by the time of charge firing. The rapid nature of this process is prevented by the conducting SCW case, in which eddy currents are induced during its motion in a magnetic field, according to the electromagnetic induction law [2], and these currents screen the liner. The level of the magnetic field penetrating into the liner depends on the residence time of the SCW in the field. Therefore, the process of magnetic-field penetration into the liner is determined not only by the spatial distribution of the field near the object being protected but also by the velocity of motion of the SCW (the greater the length of the region with the magnetic field along the SCW trajectory and the lower the SCW velocity, the higher field intensity will be attained in the liner). The dimension of the region of space with the magnetic field depends on the dimensions of the field source placed on the object being protected, and hence, on the dimensions of the object itself. The present paper analyzes the fundamental possibility of "magnetizing" a SCW liner of specified dimensions during the time it takes for the SCW to approach an object.

The magnetic-field effect on the SCJ formation during shaped-charge implosion was studied by x-ray registration.

EXPERIMENTS WITH SHAPED CHARGES IN AN EXTERNAL MAGNETIC FIELD

The present studies were using a SC 30 mm in diameter which had a conical copper liner 1 mm thick with a cone angle of 30^{o}. The magnetic field in the liner was produced by a one-turn solenoid. The magnetic-field induction in the liner at the

moment of SC firing was determined on the basis of the current curves recorded in the explosive experiments taking into account the relationship between the solenoid discharge current and the magnetic field in the liner cavity established in calibration experiments. Figure 2 gives X-ray photographs of the SCJ formed at the center of the liner at the time of liner collapse for a field induction of B_0 = 0.84 T (Fig. 2a) and

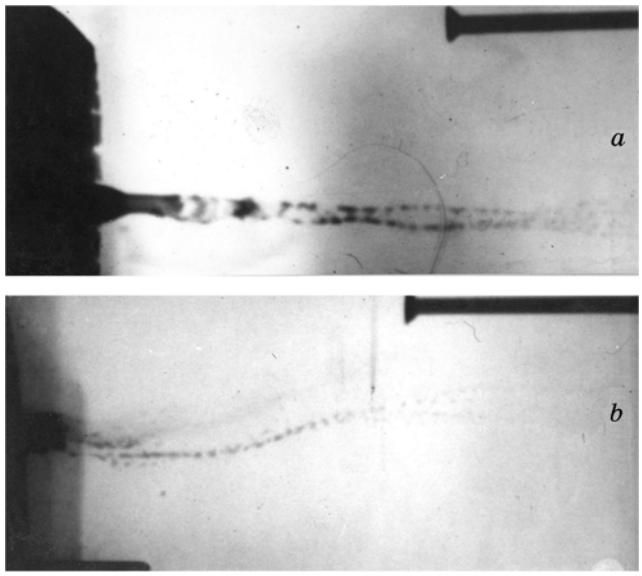

Figure 2. X-ray photographs of the shaped charge jets in a magnetic field: a) B_0 = 0.84 T, b) B_0 = 1.4 T

B_0 = 1.4 T (Fig. 2b). The recording time is the same in both cases. The X-ray photographs of the disruption pattern of the SCJ, which first takes the shape of an expanding hollow ``tube" (Fig. 2a) and is then completely dispersed (Fig. 2b), indicate an internal "explosion" in the jet, due apparently to the "pumping" of a strong magnetic field.

FORMULATION AND ANALYSIS OF THE PROBLEM

We consider a model spherical object (which is simultaneously a magnetic-field source) of radius R_0 (Fig. 3) which produces a stationary magnetic field. In the space external to the object (where other field sources are assumed to be absent), the magnetic field is potential. Introducing a scalar function $\varphi(\vec{r})$ of the field potential so that $\vec{B} = grad\varphi$ and assuming that the field produced by the spherical object is axisymmetric, for the function $\varphi(r,\theta)$ in spherical coordinates (r,θ) with origin at the center of the object we have the Laplace equation

$$\frac{1}{r^2}\frac{\partial}{\partial r}\left(r^2\frac{\partial\varphi}{\partial r}\right)+\frac{1}{r^2\sin\theta}\frac{\partial}{\partial\theta}\left(\sin\theta\frac{\partial\varphi}{\partial\theta}\right)=0\,. \qquad (1)$$

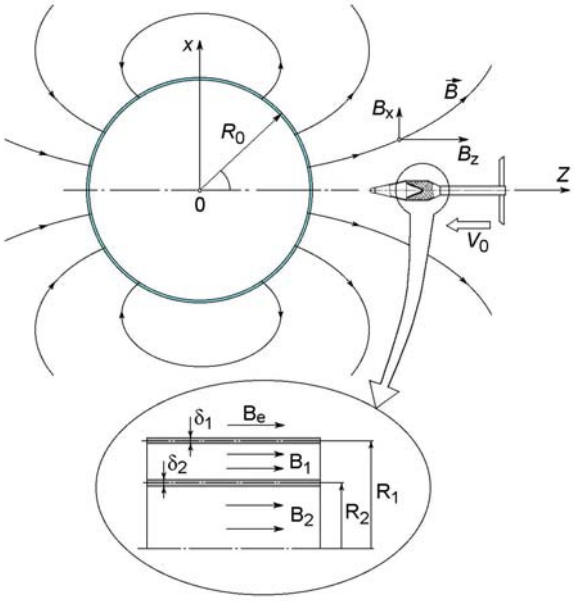

Figure 3. Computational scheme for determining the magnetic induction in a shaped-charge liner moving in a magnetic field.

The solution of this equation takes a particularly simple form if on the surface of the sphere $r = R_0$ (Fig. 3) the distribution of the radial component B_r of the magnetic-induction vector over the polar angle is specified by the expression

$$B_r(R_0, \theta) = \left.\frac{\partial \varphi}{\partial r}\right|_{r = R_0} = B_c \cos\theta, \qquad (2)$$

where B_c corresponds to the magnetic induction at the pole of the sphere ($r = R_0$, $\theta = 0$).

The solution of the formulated external Neumann problem (1), (2) for the magnetic potential $\varphi(r, \theta)$ is given by the relation $\varphi = -0{,}5 B_c R_0^3 \cos\theta / r^2$ [3], which allows the components of the magnetic-induction vector in the space surrounding the spherical object to be defined as

$$B_r = \frac{\partial \varphi}{\partial r} = B_c R_0^3 \cos\theta / r^3; \qquad B_\theta = \frac{1}{r}\frac{\partial \varphi}{\partial \theta} = 0.5 B_c R_0^3 \sin\theta / r^3 \qquad (3)$$

The magnetic field is oriented predominantly along the axis of the SCW approaching the object if the path of motion of the object is parallel to the symmetry axis *oz* of the field produced (Fig. 3). We further consider only these approach paths. In view of (3),

the distributions of the longitudinal and transverse components of the magnetic-induction vector along these paths are written as

$$B_z = \frac{B_c R_0^3}{2} \frac{2z^2 - x^2}{\left(z^2 + x^2\right)^{5/2}}; \qquad B_x \frac{3B_c R_0^3}{2} \frac{xz}{\left(z^2 + x^2\right)^{5/2}} \tag{4}$$

Here the axial coordinate z is reckoned from the center of the object and x is the radial coordinate in the cylindrical coordinate system *(x, z)*. As follows from relations (3) and (4), the magnetic-field distribution around the spherical object considered is defined by two parameters - the radius of the object R_0 and the magnetic induction B_c at the pole of the sphere. As regards the distribution of the absolute value of the magnetic induction $B = \sqrt{B_r^2 + B_\theta^2}$ directly on the sphere surface *(r* = R_0), it is maximal at the pole of the sphere ($\theta = 0$), decreases monotonically with approach to its equatorial plane, and is 50 % of the maximum value at the equator ($\theta = 90^0$).

To determine the magnetic-induction variation in the SCW liner during its motion in the specified magnetic field of the spherical object, we use the simplified computational scheme of two conducting coaxial cylindrical shells of radii R_1 and R_2 and thicknesses δ_1 and δ_2, (Fig. 3) that correspond to the SCW case and liner. The system of shells is assumed to be placed in an external axial magnetic field $B_e(t)$, whose variation with time t should apparently be determined by the distribution of the longitudinal magnetic-field component B_z (4) along the approach path of the SCW and the SCW velocity v_0

$$B_e(t) = B_z(z(t)) = \frac{B_c R_0^3}{2} \frac{2(z_0 - v_0 t)^2 - x^2}{\left((z_0 - v_0 t)^2 + x^2\right)^{5/2}}, \tag{5}$$

where the initial coordinate of the SCW z_0 ($z = z_0 - v_0 t$) is chosen at a sufficient distance from the object (where the magnetic field is virtually absent). Under the assumption of a uniform distribution of the azimuthal induction currents over the thicknesses of the shells [4], the current density in the outer shell j_1 and that in the inner shell j_2 are defined as

$$j_1 = \left(B_1 - B_e\right)/(\mu_0 \delta_1); \qquad j_2 = \left(B_2 - B_1\right)/\left(\mu_0 \delta_2\right),$$

where $\mu_0 = 4\pi \cdot 10^{-7}$ H/m is the permeability of vacuum and B_1 and B_2 are the magnetic inductions in the gap between the shells and in the cavity of the inner shell, (Fig. 3). Writing the electromagnetic induction law for each of the shells, we obtain the following system of ordinary differential equations for the evolution of the quantities $B_1$and B_2:

$$\frac{dB_1}{dt} = \frac{2\eta_1 R_1}{\mu_0 \delta_1 \left(R_1^2 - R_2^2\right)}(B_e - B_1) - \frac{2\eta_2 R_2}{\mu_0 \delta_2 \left(R_1^2 - R_2^2\right)}\left(B_1 - B_2\right); \qquad \frac{dB_2}{dt} = \frac{2\eta_2}{\mu_0 \delta_2 R_2}\left(B_1 - B_2\right),$$

where η_1 and η_2 are the resistivities of the materials of the outer and inner shells, respectively. For convenience of the subsequent analysis of the calculation results, we rewrite this system as

$$\frac{dB_1}{dt} = \frac{1}{1-\alpha^2}\left[\frac{B_e - B_1}{\tau_1} - \alpha^2 \frac{B_1 - B_2}{\tau_2}\right]; \qquad \frac{dB_2}{dt} = \frac{B_1 - B_2}{\tau_2}, \tag{6}$$

where the quantities τ_1 and τ_2 define the characteristic times of magnetic-field diffusion [4] for the outer and inner shells

$$\tau_1 = 0{,}5\mu_0 \delta_1 R_1 / \eta_1; \quad \tau_2 = 0{,}5\mu_0 \delta_2 R_2 / \eta_2, \tag{7}$$

and the dimensionless parameter α characterizes the ratio of the radii of the shells $\alpha = R_2 / R_1$.

System (6) was integrated numerically for zero initial conditions for the magnetic inductions B_1 and B_2 and the external field B_e varying according to (5). In the calculations, we considered four typical dimensions of the system of shells, having in view different SCW diameters. In all cases, it was assumed that the material of the outer shell (the SCW case) is aluminum ($\eta_1 = 2.8 \cdot 10^{-8}$ Ohm m) and that of the inner shell (shaped-charge liner) is copper ($\eta_2 = 1{,}75 \cdot 10^{-8}$ Ohm m). The dimensions of the inner shell were specified with orientation to the cross section at the mid-height of the conical shaped-charge liner (in particular, the dimensionless parameter α in system (6) was set equal to $\alpha = 0.5$). The systems of shells considered were conditionally assigned to two types of SCW (denoted below by SCW1, and SCW2). For each of the types of SCW, the Table gives the geometrical dimensions of the shells used in the calculations and the characteristic times of magnetic-field diffusion for the shells calculated by relations (7).

Table

Parameters of Equivalent Systems of Conducting Shells for Various Shaped Charges.

SC type	R_1, mm	δ_1, mm/ δ_2, mm	τ_1, ms/ τ_2, ms
SCW1	35,0	1,1 / 1,2	0,86 / 0,75
SCW2	50,0	1,6 / 1,9	1,79 / 1,70

The range of the examined velocities of approach to the object was 100 ... 400 m/s for all SCWs. Figure 4 illustrates the variation in the external field B_e (5) and the field B_2 in

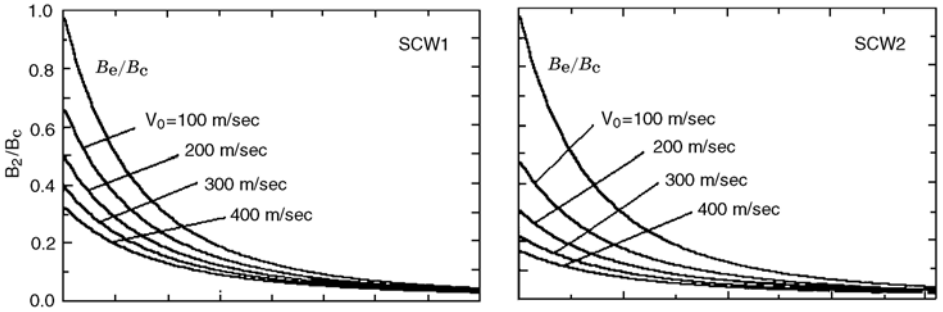

Fig. 4. Magnetic-field variation in the liners of various shaped charges approaching a spherical source along the symmetry axis

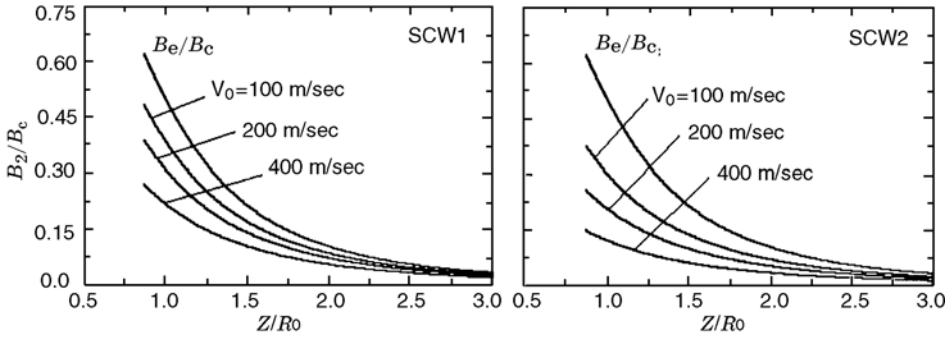

Fig. 5. Magnetic-field variation in the liner of shaped charges of diameter 70 and 100 mm approaching a spherical source along a straight line which is parallel to the symmetry axis and is separated from it by half the source radius.

the cavity of the shaped-charge liner for approaching SCWs of various types as a function of their current coordinate z with respect to the center of the spherical object (Fig. 3) for motion of the SCW along the symmetry axis of the field ($x = 0$). The radius of the spherical object (which determines the dimension of the region with the magnetic field) was set equal to $R_0 = 1$ m. As is evident from Fig. 4, an increase in the SCW velocity leads to a decrease in the induction of the field penetrating into the SCW liner. However, for SCW1 (diameter 70 mm), the liner field induction B_2 remains fairly close to the external-field induction over the entire range of approach velocities (even at a velocity $v_0 = 400$ m/sec, the value of B_2 is more than 30 % of B_e). For SCW2 (diameter 100 mm), the liner field induction at maximum velocities of motion decreases to approximately 17 % of the induction of the field produced by the object. Figure 5 illustrates the variations of the fields B_e and B_2 for SCW1 and SCW2 which approach the spherical object along a straight line that is parallel to the *0z* axis and is separated from it by a distance of $x = 0{,}5R_0$. The induction of the longitudinal magnetic field B_e (5) produced by the object on this straight line is somewhat lower than that on the

symmetry axis. As a result, by the moment of approach to the boundary of the object, the liner field induction B_2 is 25... 50 % of the maximum field B_c at the pole of the object for SCW1 and (0.15... 0.35) B_c for SCW2.

Setting $B_c \approx 1{,}5$ T in the computational scheme being analyzed, one can find (Fig. 4 and Fig. 5) that with approach to the surface of a "magnetic" sphere of radius $R_0 = 1$ m, the magnetic induction B_2 in the liner for SCW1 and SCW2 will have values not lower than 0.4 and 0.3 T, respectively. This can be sufficient to disrupt the jet and reduce its penetration into the target.

CONCLUSION

The estimation performed confirms that "magnetic screening" of objects from the SCW action is in principle possible. It should be noted that failure of the normal operation of a SC can be achieved by producing not only a longitudinal (axial) magnetic field (considered in the present paper) in its liner but also a transverse field. The generation of a magnetic field in a liner that is perpendicular to the liner axis also creates conditions for field amplification in the jet-forming layer of the liner during its collapse with the ensuing crisis of jet formation. The indicated circumstance could significantly simplify the implementation of "magnetic protection" of objects because its experimental confirmation would eliminate the need for controlling the mutual orientation of the magnetic lines of the "protective" field being produced and the axis of the approaching SCW.

The proposed nonconventional method of protecting against shaped charges may be useful for increasing the hardness of some particularly important objects (for example, storage and transportation containers for chemical or nuclear materials), for which there is a threat of terrorist attack, in particular, using hand-held antitank grenade launchers, which are available in a large quantity in terrorist groups.

REFERENCES

1. S. V. Fedorov, A. V. Babkin, and S. V. Ladov. “Influence of the magnetic field produced in the liner of a shaped charge on its penetrability”, *Combust., Expl., Shock Waves,* **35**, No. 5, 598-609, (1999).
2. S. V. Fedorov, A.V. Babkin, S.V. Ladov, G.A. Shvetsov, A.D. Matrosov and A.G. Anisimov “Magnetic field amplification in high-velocity metal jets from explosions”, *Proc. of Int. Workshop “High Energy Density Hydrodynamics”*, ed by G.A. Shvetsov, Novosibirsk, 2003, pp. 183-204.
3. A. N. Tikhonov and A. A. Samarskii. “Equations of Mathematical Physics [in Russian]”, Nauka, Moscow (1966).
4. H. Knoepfel. “Pulsed High Magnetic Fields”, North-Holland, Amsterdam, (1970).